

Supplementary Information for:

Extraction of Chlorobenzenes and PCBs from Water by ZnO Nanoparticles

Yuntao Zhang,[†] Ran Chen,[†] Jim E Riviere[†] and Jeffrey Comer^{*†}

* Corresponding author. Email: jeffcomer@ksu.edu

[†]Institute of Computational Comparative Medicine, Nanotechnology Innovation Center of Kansas State, Department of Anatomy and Physiology, Kansas State University, Manhattan, Kansas, 66506-5802

Table of Contents

Supplementary Methods

References for Supplementary Methods

Table S1. Physicochemical characterization of the ZnO particles used in this study.

Table S2. Optimized GC/MS/MS parameters.

Table S3. Qualifier and quantifier MRM transitions and optimum parameters for the aromatic organochlorines.

Table S4. Limits of quantification and linear ranges of the aromatic organochlorides.

Figure S1. Representative MRM spectrum of the aromatic organochlorides.

Figure S2. Convergence of the free energy calculations.

Figure S3. Differences between free energy profiles for chlorobenzene isomers and associated uncertainties.

Figure S4. Contribution of Cl atoms of the aromatic organochlorides to their interaction with ZnO NPs at different nanoparticle concentrations.

Supplementary Methods

Reactive Molecular Dynamics Simulations of ZnO. To choose the atomic structure of the ZnO surface, we melted ZnO nanoparticles at 2500 K in vacuum and cooled them to room temperature over 3 ns in simulations using the ReaxFF force field [1]. The resulting nanoparticles adopted the wurzite crystal structure, consistent with x-ray diffraction

characterization of the ZnO NPs used in the experiments [2], and exhibited a clear preference for free surfaces consisting of the Zn-terminated $\{0001\}$ crystallographic plane [3]. Further simulation of these structures in water at standard conditions showed the formation of metal hydroxyls on undercoordinated Zn and O atoms on steps between $\{0001\}$ planes and for other exposed facets (such as the $\{10\bar{1}0\}$ crystal plane) [4]. However, the Zn-terminated $\{0001\}$ faces exhibited no chemical reconstruction when exposed to water in simulation. Due to the apparent preference for this crystal plane, in all subsequent simulations, the surfaces of the ZnO NPs were modeled by flat Zn-terminated $\{0001\}$ faces. Our model should approximate nanoparticles with surfaces that are roughly flat on the length scale of the PCBs (≈ 1 nm). Although the ZnO NPs appear approximately spherical [2], the transmission electron images are consistent with local flatness at this length scale.

Optimization of ZnO Parameters. The search of parameters for the ZnO atoms covered the following domains: $1.2 \leq R_{\text{Zn}}/2 \leq 1.6$ Å, $0.05 \leq \epsilon_{\text{Zn}} \leq 0.5$ kcal/mol, $1.5 \leq R_{\text{O}}/2 \leq 1.8$ Å, $0.05 \leq \epsilon_{\text{O}} \leq 0.3$ kcal/mol, and $0.1 \leq Q \leq 1.0$ e, where R is the distance associated with the minimum Lennard-Jones energy, ϵ is the minimum Lennard-Jones energy, and Q and $-Q$ are the partial charges of the ZnO zinc and oxygen atoms in elementary units. In CHARMM format parameter files, half the distance associated with minimum Lennard-Jones energy ($R/2$) is listed in the NONBONDED section and so we report those values here. The adsorption coefficients ($\log k$) were calculated as described in the main text. We sought to find the parameters that best reproduced the experimental difference in the logarithm of the equilibrium constant between two compounds, biphenyl and 2,3-dichlorobiphenyl ($\Delta L = \log_{10}(k_{\text{PCB5}}/k_{\text{PCB0}})$). The search was stopped when $|\Delta L_{\text{sim}} - \Delta L_{\text{expt}}| < 0.1$. After performing calculations for 72 parameter sets, the stopping criterion was met for $R_{\text{Zn}}/2 = 1.5$ Å, $\epsilon_{\text{Zn}} = 0.28$ kcal/mol, $R_{\text{O}}/2 = 1.75$ Å, $\epsilon_{\text{O}} = 0.08$ kcal/mol, and $Q = 0.15$ elementary units. This parameter set was used for all calculations described in the Results and Discussion.

Supplementary Methods References

1. Raymand, D.; van Duin, A. C.; Baudin, M.; Hermansson, K. *Surf. Sci.* **2008**, *602*, 1020–1031.
2. Chen, R.; Zhang, Y.; Darabi Sahneh, F.; Scoglio, C. M.; Wohlleben, W.; Haase, A.; Monteiro-Riviere, N. A.; Riviere, J. E. *ACS Nano* **2014**, *8*, 9446–9456.
3. Nawrocki, G.; Cieplak, M. *Phys. Chem. Chem. Phys.* **2013**, *15*, 13628–13636.
4. Thomas, S. E.; Comer, J.; Kim, M. J.; Marroquin, S.; Murthy, V.; Ramani, M.; Hopke, T. G.; McCall, J.; Choi, S.-O.; DeLong, R. K. *Int. J. Nanomedicine* **2018**, *2018*, 4523–4536.

Table S1. Physicochemical characterization of the ZnO particles used in this study. Methods of characterization the nanomaterials have been documented (see Ref. 2 in Supplementary Methods References above).

| ZnO particles | Primary particle size (TEM, nm) | Dynamic light scattering in distilled water (DLS, nm) * | Zeta-potential in distilled water (mV) * | Specific surface area (BET, m ² /g) | Surface coating |
|---------------|---------------------------------|---------------------------------------------------------|------------------------------------------|------------------------------------------------|-----------------|
| 1 | 14 | 367 | -23 | 30 | None |
| 2 | 80 | 217 | -18 | 12 | None |
| 3 | 1000 | 2208 | -14 | 5 | None |

* The concentration of the ZnO particles in distilled water is 100 mg/L.

Table S2. Optimized GC/MS/MS parameters.

| | GC system |
|---------------------------------------------------------------------------------------------------------------------------------------------|-----------------------------------------------------------------------------------------------------------------------------------------------------------------------------------------------------------------------------------------------------------------------------------------|
| Capillary column Carrier gas Inlet Inlet temperature Injection mode Injection pulse pressure Oven profile | Agilent 30 m × 0.25 mm (i.d.) × 0.25 μm (df) HP-5MS Helium, constant pressure at 85 psi Multi-mode inlet 280 °C Pulsed splitless mode 36 psi until 1 min 40 °C for 2 min, to 150 °C at 25 °C /min, to 200 °C at 5 °C /min, to 280 °C at 10 °C /min and hold for 5 min |
| | MS/MS system |
| MS mode Transfer line temperature Ion source temperature Quad temperature Solvent delay Collision gas flows MS resolution | MRM 280 °C 230 °C Q1 and Q2 = 150 °C 3.75 min Helium quench gas at 2.35 ml/min, N ₂ collision gas at 1.5 ml/min MS1 and MS2 = 1.2 amu (Wide setting) |

Table S3. Qualifier and quantifier MRM transitions and optimum parameters for the aromatic organochlorines.

| Peak # on chromatogram | Compound name | Retention time (min) | Precursor ion | MRM ion | Optimum Dwell (ms) | Optimum Collision (V) |
|------------------------|---------------------|----------------------|---------------|---------|--------------------|-----------------------|
| 1 | Monochlorobenzene | 4.2 | 111.9 | 77 | 10 | 15 |
| 2 | Dichlorobenzene | 5.676 | 145.9 | 110.9 | 10 | 20 |
| 3 | Trichlorobenzene | 6.551 | 179.8 | 144.9 | 10 | 20 |
| 4 | Tetrachlorobenzene | 8.107 | 215.8 | 180.9 | 10 | 30 |
| 5 | Monochlorobiphenyl | 9.85 | 187.9 | 151.9 | 10 | 30 |
| 6 | Pentachlorobenzene | 10.173 | 249.8 | 214.8 | 10 | 20 |
| 7 | Dichlorobiphenyl | 12.657 | 221.9 | 151.9 | 10 | 30 |
| 8 | Hexachlorobenzene | 12.884 | 283.7 | 248.7 | 10 | 25 |
| 9 | Trichlorobiphenyl | 14.993 | 255.8 | 185.9 | 10 | 30 |
| 10 | Tetrachlorobiphenyl | 16.854 | 291.8 | 219.9 | 10 | 30 |
| 11 | Pentachlorobiphenyl | 18.447 | 325.8 | 253.8 | 10 | 35 |
| 12 | Hexachlorobiphenyl | 20.06 | 359.7 | 289.8 | 10 | 35 |
| 13 | Heptachlorobiphenyl | 22.773 | 393.7 | 323.8 | 10 | 35 |
| 14 | Octachlorobiphenyl | 22.901 | 429.7 | 357.7 | 10 | 35 |
| 15 | Nonachlorobiphenyl | 25.668 | 463.7 | 391.7 | 16.5 | 40 |
| 16 | Decachlorobiphenyl | 26.38 | 497.6 | 427.7 | 16.5 | 40 |

Table S4. Limits of quantification and linear ranges of the aromatic organochlorides.

| # | Organochlorides | Quantification RSD (%) | LOQ (mg/L) | R2 (LOQ - 1×10^{-1} mg/L) | Recovery (%) |
|----|---------------------|------------------------|--------------------|------------------------------------|--------------|
| 1 | Chlorobenzene | 0.9928 | 1×10^{-3} | 0.9958 | 98.8 |
| 2 | Dichlorobenzene | 2.3258 | 1×10^{-3} | 0.9889 | 99.3 |
| 3 | Trichlorobenzene | 0.7057 | 1×10^{-3} | 0.9921 | 98.8 |
| 4 | Tetrachlorobenzene | 0.3441 | 1×10^{-3} | 0.9939 | 96.2 |
| 5 | Monochlorobiphenyl | 2.9029 | 1×10^{-3} | 0.9878 | 98.1 |
| 6 | Pentachlorobenzene | 7.0268 | 1×10^{-3} | 0.9933 | 96.8 |
| 7 | Dichlorobiphenyl | 7.4356 | 1×10^{-3} | 0.9910 | 98.6 |
| 8 | Hexachlorobenzene | 3.1412 | 1×10^{-3} | 0.9909 | 95.9 |
| 9 | Trichlorobiphenyl | 5.2179 | 1×10^{-3} | 0.9951 | 97.3 |
| 10 | Tetrachlorobiphenyl | 11.8341 | 1×10^{-3} | 0.9947 | 96.9 |
| 11 | Pentachlorobiphenyl | 6.1419 | 1×10^{-3} | 0.9964 | 94.6 |
| 12 | Hexachlorobiphenyl | 5.2029 | 1×10^{-3} | 0.9957 | 95.5 |
| 13 | Heptachlorobiphenyl | 9.5084 | 1×10^{-3} | 0.9962 | 94.9 |
| 14 | Octachlorobiphenyl | 11.0021 | 1×10^{-3} | 0.9948 | 97.4 |
| 15 | Nonachlorobiphenyl | 6.4700 | 1×10^{-3} | 0.9950 | 96.1 |
| 16 | Decachlorobiphenyl | 6.8030 | 1×10^{-3} | 0.9940 | 93.8 |

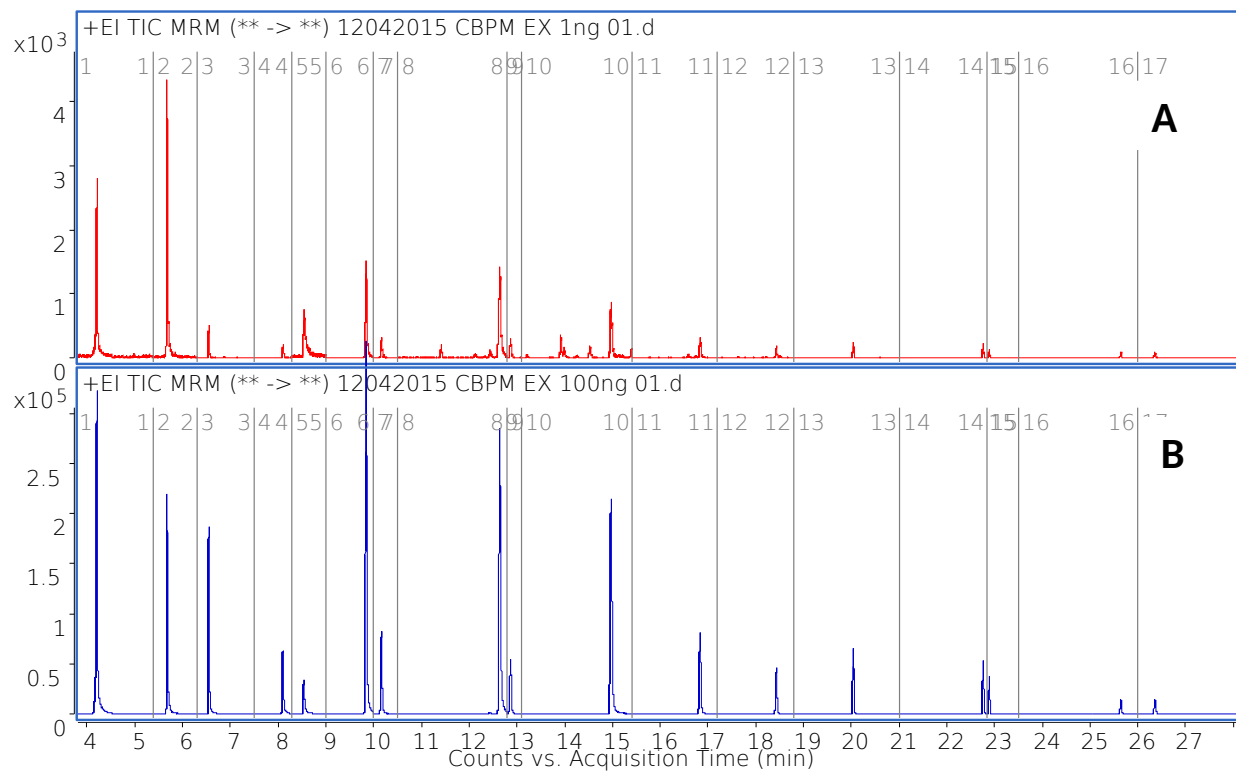


Figure S1. Representative MRM spectrum of the aromatic organochlorides. **(A)** The concentrations of organochlorides at 1×10^{-3} mg/L. **(B)** The concentrations of organochlorides at 1×10^{-1} mg/L.

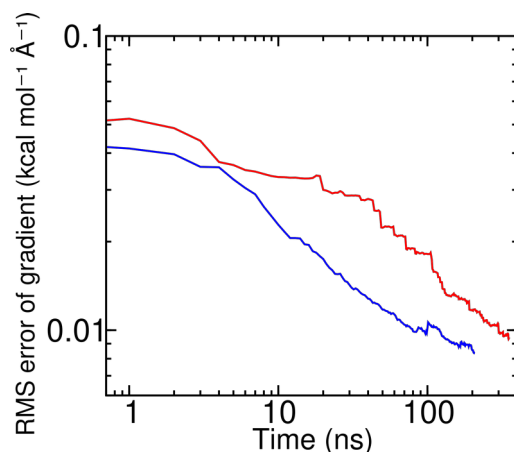


Figure S2. Convergence of the free energy calculations. Example of the convergence of the mean force along the transition coordinate (Z) in two different ABF simulations toward the reference mean force obtained from a third long ABF simulation (600 ns). This example is for adsorption of PCB 2 onto the ZnO surface in water.

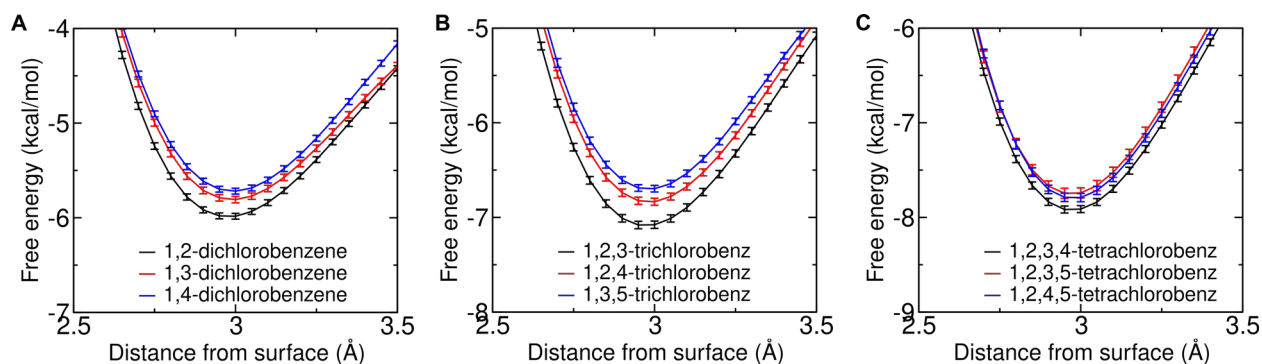


Figure S3. Differences between free energy profiles for chlorobenzene isomers and associated uncertainties. (A–C) plots of free energy minima for dichlorobiphenyl (A), trichlorobiphenyl (B), and tetrachlorobiphenyl (C). Uncertainties (error bars) are computed by partitioning mean force samples into the those from the first half of the simulation and those from the second half of the simulation. The uncertainty of the gradient at each ABF bin is taken to be the absolute difference between the mean force for that bin between the two halves. The uncertainty in the potential of mean force is then calculated by integrating over the mean force uncertainties, beginning from the region where the potential of mean force is anchored ($Z = 13.75$ Å).

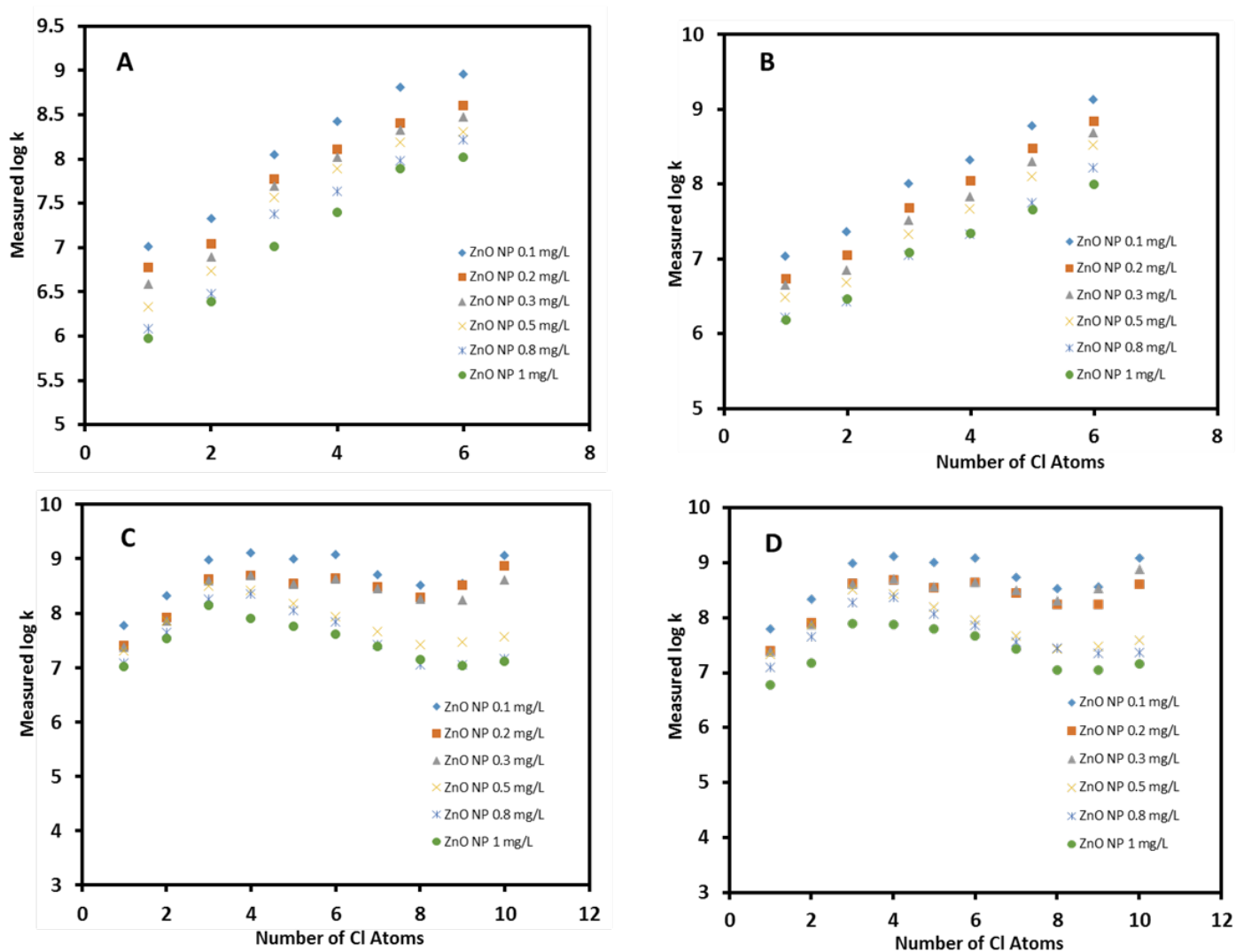


Figure S4. Contribution of Cl atoms of the aromatic organochlorides to their interaction with ZnO NPs at different nanoparticle concentrations. (A) Concentrations of the chlorobenzenes at 1×10^{-2} mg/L. (B) Concentrations of the chlorobenzenes at 5×10^{-2} mg/L. (C) Concentrations of the chlorobiphenyls at 1×10^{-2} mg/L. (D) Concentrations of the chlorobiphenyls at 5×10^{-2} mg/L.